IGARSS 2024 - 2024 IEEE International Geoscience and Remote Sensing Symposium | 979-8-3503-6032-5/24/$31.00 ©2024 IEEE | DOI: 10.1109/IGARSS53475.2024.10641907

CARDINAL EFFECT IN BISTATIC SAR IMAGERY: ANALYSIS AND PHYSICAL INTERPRETATION

Gerardo Di Martino, Alessio Di Simone, Antonio Iodice, Daniele Riccio, Giuseppe Ruello

Department of Electrical Engineering and Information Technology,
University of Naples Federico II, 80125 Naples, Italy

ABSTRACT

This paper is aimed at supporting the analysis and interpretation of bistatic synthetic aperture radar (SAR) images, which are available by now through the Capella constellation or will be soon available thanks to the upcoming PLATiNO-1 mission. More specifically, here we focus on urban areas, where the so-called *cardinal effect* dominates the backscattering in conventional monostatic SAR imagery. Such effect is also evident in bistatic acquisition geometries, as it has been recently demonstrated, even if with different dynamics. Through the application of analytical models for the electromagnetic scattering from buildings in bistatic geometries, we provide a physical explanation of the SAR image formation in the urban environment and in arbitrary acquisition geometries. We quantitatively evaluate the contrast between the returns from the building and the surrounding terrain under different roughness regimes and imaging geometries. The analyses provided here might support a correct human interpretation and automatic processing of urban bistatic SAR images.

Index Terms— bistatic SAR, electromagnetic scattering, physical optics, multistatic geometry, CubeSats

1. INTRODUCTION

It is well known that synthetic aperture radar (SAR) images of urban areas exhibit strong linear patterns which are associated to the double-bounce scattering arising from the interaction between the buildings walls and the surrounding ground. Such effect is known as the *cardinal effect*, first noted in SAR imagery by Levine in 1960 [1] and is typically also referred to as the *corner reflector effect* within the SAR community.

This phenomenon is particularly evident in monostatic SAR images when linear man-made structures, e.g., buildings or bridges, are parallel to the sensor line of flight. In this case, trough a simple ray-optics approach, it can be demonstrated that electromagnetic (EM) waves impinging upon the linear structure are specularly reflected towards the ground and, then, mostly reflected back to the sensor. As a result, a very strong linear EM echo, compared to background signal, appears in the SAR image in correspondence of the structure base. Therefore, SAR images appear extremely bright in urban areas, compared to other scenarios, e.g., bare soil, vegetated areas, sea.

While the cardinal effect might be properly exploited to retrieve geometric information about the building, e.g., its height [2], it might be detrimental to a comprehensive information retrieval in urban areas, as the strong double-bounce component might mask objects in the vicinity of the building due to image saturation. This has motivated the development of techniques for cardinal effect reduction in urban SAR imagery [3].

In the last two decades, spaceborne bi- and multi-static SAR systems have been conceptualized and proven to enable innovative imaging modes and applications [4], such as tomography. TanDEM-X is a bistatic spaceborne SAR formation and has been providing bistatic SAR imagery from space since 2010, even though with along- and cross-track baselines as limited as 1 km or below. More recently, the Capella Space company proved bistatic SAR imaging capabilities and the first SAR image acquired from a spaceborne bistatic configuration with a large bistatic angle has been acquired [5]. Additionally, some spaceborne missions, e.g., PLATiNO-1 operated by the Italian Space Agency (ASI), are planned to offer systematic bistatic SAR acquisitions in the near future [6]. Distributed spaceborne SAR, e.g., formation-flying SAR, implemented through multi-static small platforms, e.g., CubeSats, represents a further innovative imaging concept in the field of Earth observation from space [7]. This paper investigates, from a physical-based perspective, the cardinal effect in spaceborne bistatic SAR imagery under different acquisition geometries and scene characteristics. The paper is organized as follows: Section 2 describes the bistatic SAR systems analyzed; Section 3 briefly recalls the EM scattering models adopted in support of our investigations; Section 4 shows the simulation results; Section 5 highlights the main conclusions.

2. BISTATIC SAR SYSTEMS

Here we describe the SAR missions that demonstrated or are planned to offer bistatic imaging capabilities from space, i.e., the Capella Space constellation and the ASI PLATiNO-1.

2.1. Capella Space constellation

Capella Space is one of the first commercial companies to design, launch, and operate a constellation of satellites with SAR imaging capabilities. The first satellite of the constellation was launched in 2020, and many other platforms have been launched over the last years. The final constellation consists of 36 sub-50 kg satellites, orbiting at an altitude of around 500 km in polar orbits and providing revisit times of less than one hour, on average [8].
Each satellite of the constellation is equipped with a SAR payload working at X-band (9.65 GHz), single-pol, and implementing stripmap, spotlight and sliding spotlight acquisition modes [8]. Radar parameters, e.g., bandwidth, azimuth resolution, number of looks, polarization, are customizable. The very high resolution down to 0.5 m, will enable interferometric measurements in urban areas thanks to the possibility to resolve urban structures.
SAR imagery products are made available to approved Capella Console users at no cost through the Capella Open Data Program [8].

2.1.1. Capella Bistatic SAR Imaging Experiment

Very recently, Capella Space announced the launch of a new generation of satellites that will offer enhanced imaging capabilities with a bandwidth of 700 MHz and will enable advanced SAR products, among which bistatic imaging [5]. An experimental activity of bistatic SAR imaging has been carried out on March 31, 2023 over Punta Alta, Argentina and is detailed in [5]. During the acquisition time, a satellite performed a regular 20 s spotlight imaging task, while another satellite was activated on a receive-only mode while steering its antenna towards the sensed scene. The two satellites were separated by about 275 km with a bistatic angle of around 30° [5]. After multilooking, the final bistatic image has a spatial resolution of 0.5 m × 0.5 m. An image cut over the Hotel Puerto Belgrano and the full image can be found in [5] and [9], respectively, where the monostatic acquisition is shown as well for comparison. The observed scene includes an urban area and some isolated buildings and is, therefore, suitable for appreciating the cardinal effect on a real bistatic SAR image. Apart from obvious differences related to scene rotation and feature size due to the different squint angles and image coordinate systems involved in the two acquisitions, the bistatic image still differs substantially from the monostatic one. Indeed, as noted in [5], urban structures appear more brilliant in the bistatic image (see e.g., the Hotel Puerto Belgrano in the top-middle of the whole scene and the residential area in the leftmost area), while they are hardly visible, apart from a few brilliant points or lines, in the monostatic one. In general, the whole scene, including vegetated and bare soils, appears relatively brighter in the bistatic acquisition than the monostatic one, the only exception being the wetland area close to Puerto Belgrano in the rightmost region of the image, thus potentially revealing a lower dynamic range of the bistatic measurements. However, it is worth noting that such considerations can be derived from a pure visual comparison as neither monostatic nor bistatic SAR calibrated experimental data are made available from Capella Space company at date.

2.2. PLATiNO-1

PLATiNO-1 is an upcoming spaceborne mini-satellite SAR mission designed by ASI within the Earth Observation PLATiNO programme and planned to be launched by the end of 2024 [6]. It will operate in X-band and will ensure full compatibility with CosmoSkyMed, both 1st and 2nd generation, also known as CSK and CSG, respectively. Indeed, in the first operational phase, PLATiNO will orbit in formation with one CSK/CSG satellite at the same altitude of about 619 km and will mainly work as a receiver acquiring the Earth-reflected signal transmitted by CSK/CSG. In this phase, it will implement a passive bistatic SAR where CSK/CSG signals will be opportunistically exploited for remote sensing purposes. In the second operational phase, PLATiNO-1 will be re-orbited on a lower orbit, at about 410 km altitude, where it will mainly operate as a conventional monostatic SAR.
In both phases, SAR images will be acquired in the standard stripmap mode at a resolution of 3 m [10].

3. THEORETICAL BACKGROUND

To quantitatively evaluate the cardinal effect in bistatic SAR imagery, here we rely on closed-form EM scattering models suited to bistatic geometries and to the urban environment. More specifically, we adopt the scattering formulations described in [11], [12], which focus on the evaluation of microwave scattering from a canonical building. The geometry of the scattering problem is sketched in Figure 1: the transmitter is located in the *z*-*y* plane, so that $\vartheta_s = \vartheta$ and $\varphi_s = \pi/2$ define a backscattering geometry, while $\varphi \in]-\pi/2, \pi/2]$ is the angle between the positive *x*-semiaxis and the longest wall base. Accordingly, if $\varphi = n\pi/2$, with $n = 0,1$, the building is faced towards the Tx sensor. In all the above-mentioned works, the observed scene comprises a canonical building, modeled as a parallelepiped with smooth dielectric faces, lying over a background surface modelling terrain or asphalt and described as a random rough surface. The coherent (i.e., mean EM field) and incoherent (i.e., EM field variance) components of the scattered field are evaluated within the framework of the Kirchhoff Approximation (KA) and subsequent Geometrical Optics (GO) and Physical Optics (PO) solutions. Accordingly, the EM field scattered from each wall of the building is expressed as the superposition of the following multiple-bounce components, see Figure 2:

- one single-scattering term from the building roof;
- two double-scattering (wall-ground and ground-wall) terms comprising one reflection on the building wall and one reflection on the ground;

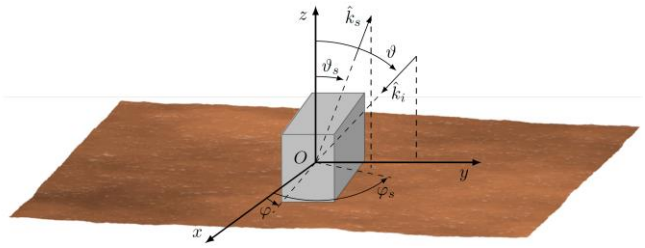

Figure 1: Reference system for the building scattering problem.

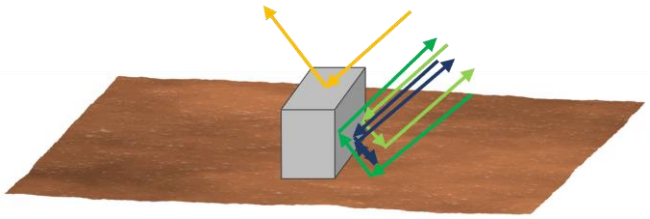

Figure 2: Multiple-bounce contributions: single-scattering from roof (yellow), double-scattering wall-ground (light green), double-scattering ground-wall (dark green), triple-scattering wall-ground-wall (blue).

- one triple-scattering term (wall-ground-wall), comprising two reflections from the wall and one from the ground.

The overall EM field scattered from the whole building is the superposition of the contributions from the single walls.

It is worth mentioning that the single-scattering component from the building roof is mostly concentrated in the specular reflection direction and, hence, cannot be appreciated in both monostatic SAR and bistatic SAR systems working in far-from-specular geometries. Additionally, the triple-scattering contribution, despite being mostly focused in directions close to the backscattering one, is scarcely visible in SAR imagery due to the triple reflection.

As a result, the scattering from a canonical building in far-from-specular directions is dominated by the double-scattering components in both monostatic and bistatic imaging geometries [11].

Reflections from the building wall are described via GO due to surface smoothness, while scattering from the rough ground is described via GO [11], or PO [12], the choice depending upon the roughness of the underlying surface, which is described as an isotropic surface. Such an approach allows for keeping the mathematical treatability of the problem, and, hence, for formulating the scattered field statistics through closed-form expressions.

With reference to the coherent component of the double-scattering field (appreciable only under gentle roughness conditions, i.e., under PO approximation), it is helpful to recall here that the maximum scattered power is attained in $\vartheta_s = \vartheta$ and $\varphi_s = \pi/2 - 2\varphi$ [11], the latter condition defining the local maximum in terms of φ for a fixed imaging geometry, i.e., for fixed ϑ, ϑ_s, and φ_s. Accordingly, in the backscattering case, i.e., $\vartheta_s = \vartheta$ and $\varphi_s = \pi/2$, the strongest return is attained if $\varphi = n\pi/2$, with $n = 0,1$, i.e., if a building wall is faced towards the Tx sensor.

Table I: Simulation parameters.

Parameter	**Value**
Frequency	9.6 GHz
Polarization	HH
Incidence angle	30°
Altitude	500 km
Tx-Rx distance	see *Table II*
Building size	L 30 × W 20 × H 30 m^3
Ground surface rms height	0.0032 m (Scenario A) 0.04 m (Scenario B)
Ground surface correlation length	0.048 m (Scenario A) 0.3 m (Scenario B)
Building dielectric const.	4 – j0.1
Ground dielectric const.	4 – j0.1

Table II: Bistatic configurations with ground NRCS.

Tx-Rx distance (km)	ϑ_s (deg.)	φ_s (deg.)	Ground NRCS (dB) – A/B
0	30.00	90	-32.30/-33.26
20	30.06	93.96	-32.33/-33.33
100	31.43	109.11	-33.24/-34.80
275	38.57	133.61	-38.04/-43.29
500	49.11	150.00	-45.32/-58.96

4. PHYSICAL INTERPRETATION

The bistatic SAR returns from urban areas is here investigated by evaluating the contrast, i.e., the ratio, between the radar cross section (RCS) of an isolated building and that of the surrounding ground surface. Two different scenarios are considered:

- Scenario "A": the ground surface is slightly rough, with a RMS slope of 0.0943. PO and GO-PO models are adopted to describe the ground surface scattering and the multiple-bounce building scattering [12].
- Scenario "B": the ground surface is very rough with a RMS slope of 0.189 and with ground surface rms height larger than EM wavelength. GO and GO-GO models are adopted to describe the ground surface scattering and the multiple-bounce building scattering [11].

Simulation parameters are reported in Table I and are consistent with the SAR missions described in Section 2, while the considered bistatic imaging configurations are listed in Table II along with the normalized RCS (NRCS) of the ground surface in both scenarios. In the considered analysis, Tx and Rx are on the same orbit which is parallel to the *x*-axis. From Table II, it emerges that the ground NRCS decreases with increasing Tx-Rx distance, i.e., with increasing bistatic angle. Building-to-ground RCS ratio (BGR) is shown in Figure 3 and Figure 4 as a function of the building orientation angle φ for the different bistatic configurations, including the one described in Section 2.1.1, and for the gentle and very rough scenarios, respectively.

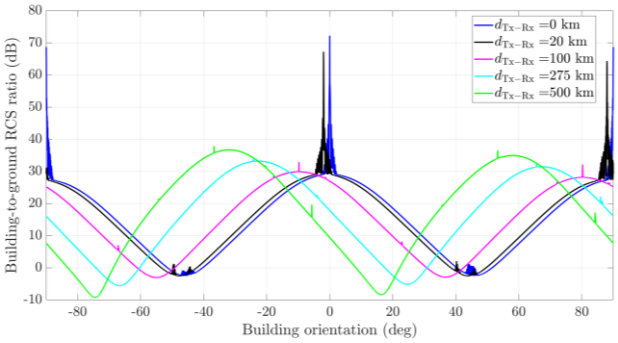

Figure 3: Building-to-ground RCS ratio in dB vs building orientation for different Tx-Rx baselines with slightly rough terrain (scenario A). Ground scattering is described via PO.

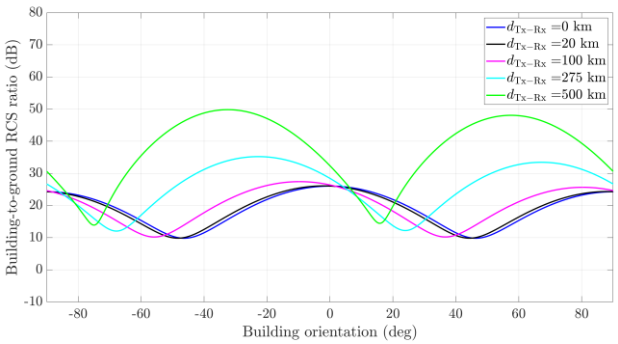

Figure 4: Building-to-ground RCS ratio in dB vs building orientation for different Tx-Rx baselines with very rough terrain (scenario B). Ground scattering is described via GO.

As it would be expected, BGR depends upon the building orientation and the lobes are representative of the incoherent scattering component of rough ground-walls double bounces. With low Tx-Rx distance, i.e., small bistatic angles, the largest BGR values are obtained with the building facing the Tx. If, additionally, the building is placed over a smooth terrain (e.g., asphalt), the coherent component of the double-bounce term is clearly visible and largely dominates BGR at small orientation angle (see the "spikes" in Figure 3).

With increasing Tx-Rx distance, the orientation angle corresponding to maximum BGR shifts due to the specular reflections from the walls. In addition, spikes due to the coherent component disappear, but, apart from this, higher values of BGR are generally obtained, especially with very rough ground, see Figure 4. This is mainly due to the decreasing terrain NRCS with increasing bistatic angle.

These results are in agreement with the features of the images described in Sect. 2.1.1: urban areas are generally brighter in the bistatic than in the monostatic image, apart from a few brilliant points or lines in the monostatic image, most likely due to the coherent component of double bounces.

5. CONCLUSION

In this paper, we provided a quantitative evaluation of the so-called cardinal effect in bistatic SAR imagery. To this end, we relied on GO- and PO-based analytical models to describe the bistatic scattering from isolated buildings and the surrounding ground. The adopted scattering formulas account for the different multiple-bounce scattering contributions arising from the EM interactions between the building and the ground, including the double-bounce term, which is the dominant term in both monostatic and bistatic far-from-specular acquisition geometries. The analyses revealed that the orientation angle giving the largest BGR depends on the imaging geometry and that bistatic geometries might lead to enhanced BGRs w.r.t. the monostatic one, especially in presence of very rough terrain.

6. ACKNOWLEDGMENT

This work was supported by the Italian Space Agency through the Project "SimulAzione e Modellazione del Sistema BistAtico COSMO-SkyMed/Platino (SAMBA)".

7. REFERENCES

[1] D. Levin, *Radargrammetry*, McGraw-Hill Book Co., New York, NY, USA, 1960.

[2] R. Guida, A. Iodice, D. Riccio, "Height retrieval of isolated buildings from single high-resolution SAR images," *IEEE Trans. Geosci. Remote Sens.*, vol. 48, no. 7, pp. 2967-2979, Jul. 2010.

[3] W. K. Lee, "Reduction of cardinal effects in SAR imagery of densely populated urban areas by suppressing strong multiple returns," *2001 IEEE IGARSS*, vol. 5, pp. 2328-2330, Sydney, NSW, Australia, 2001.

[4] G. Krieger and A. Moreira, "Spaceborne bi- and multistatic SAR: potential and challenges", *IEE Proceedings - Radar, Sonar and Navigation*, vol. 153, no. 3, pp. 184-198, June 2006.

[5] G. Farquharson *et al.,* "The New Capella Space Satellite Generation: Acadia," *2023 IEEE IGARSS*, Pasadena, CA, USA, 2023, pp. 1513-1516.

[6] V. Stanzione, B. Sabatinelli, "Platino Project: A new italian multi-application small satellite platform for highly competitive missions", *69th International Astronautical Congress*, Bremen, Germany, 1–5 Oct. 2018.

[7] G. Di Martino *et al.* "Efficient Processing for Far-From-Transmitter Formation-Flying SAR Receivers," *IEEE Trans. Geosci. Remote Sens.,* vol. 61, pp. 1-19, 2023, Art no. 5211419.

[8] G. Farquharson *et al.* "The Capella Synthetic Aperture Radar Constellation," *2018 IEEE IGARSS*, Valencia, Spain, 2018, pp. 1873-1876.

[9] Jisu Ryu and Yuriy Goncharenko, "Capella R&D Team Demonstrates Bistatic Collect Capability," https://www.capellaspace.com/capella-space-rd-team-demonstrates-bistatic-collect-capability, 2023, [Online; accessed 13-Dec-2023].

[10] eoPortal, "PLATiNO Minisatellite Platform," https://www.eoportal.org/satellite-missions/platino#platino-1, 2023, [Online; accessed 18-Dec-2023].

[11] A. Di Simone *et al.*, "Analytical Models for the Electromagnetic Scattering From Isolated Targets in Bistatic Configuration: Geometrical Optics Solution," *IEEE Trans. Geosci. Remote Sens.*, vol. 58, no. 2, pp. 861-880, Feb. 2020.

[12] G. Di Martino *et al.*, "Bistatic scattering from a canonical building," *2020 IEEE Radar Conference (RadarConf20)*, Florence, Italy, 2020, pp. 1-6.